ISSN 2447-6102

Article

Development And Validation Of A Low-Cost Dynamic Phantom For Quality Control Of Respiratory Management Systems

Reis, R.G. [1,*], Zaratim, G. R. R[2], De Oliveira, L. M. D.[3], Da Fonseca, V. G.[3], Oliveira e Silva, L.F.[2] and Luz, G. V. S[4]

1 Hospital Universitário de Brasília, Brasília, Brasil; reis.ricardo@ebserh.gov.br
2 Confiar – Radioterapia, Goiânia, Brasil.
3 Universidade de Brasília, Brasília, Brasil.
4 Programa de Pós-graduação em Engenharia Biomédica-PPGEB, Faculdade do Gama - UNB, Brasília, Brasil.
* Correspondence: reis.ricardo@ebserh.gov.br

Received: 30/05/2025; Accepted: 03/06/2025; Published: 10/06/2025

Abstract: This study aims to develop and validate a cost-effective dynamic phantom designed to simulate respiratory motion for use in the quality control of management systems. The phantom was constructed using polycarbonate material and a Nema 17 motor to replicate respiratory motion. A user-friendly graphical interface was developed to configure movement patterns. A paraffin semi-sphere was incorporated to mimic breast anatomy, and its dimensions were verified for electronic equilibrium. System calibration adjusted the amplitude of the simulated respiratory motion based on the motor's step count. Repeatability and reproducibility tests were conducted for amplitude, apnea duration, and various frequencies. The density of the paraffin buildup cap was assessed using Hounsfield Units (HU) in Treatment Planning Systems. The movement calibration yielded a third-degree polynomial fit (R^2 = 0.999). Repeatability tests in free-breathing mode showed an average amplitude of 31.2 ± 0.17 mm, with a global relative deviation of 0.5%. Reproducibility tests revealed variances relative to the mean of less than 0.5%. In apnea mode, the maximum relative variation in movement suspension time was 0.8%. Amplitude consistency tests indicated reliable performance with variations below 0.18 mm for amplitudes above 10 mm. The paraffin cap's HU value averaged -215 ± 40, sufficient for electronic equilibrium. The developed phantom has been validated as an effective tool for conducting prescribed tests to evaluate the quality and performance of respiratory management systems. Its high precision makes it suitable for various assessments, including dosimetric evaluations and the simulation of different respiratory cycles.

Keywords: Deep inspiration breath-hold, gated radiotherapy, respiratory-gated, treatment, respiratory monitoring system, dynamic phantom.

1. Introduction

Respiratory motion significantly impacts tumors located within the thoracic and abdominal regions. This motion exhibits daily fluctuations in magnitude, periodicity, and consistency, representing a substantial source of uncertainty for the treatment of these neoplasms (Shirato et al., 2004). Furthermore, both tumors and normal tissues have the capacity to undergo contraction, expansion, and repositioning in response to radiation therapy and potentially concurrent therapies (Keall et al., 2006). In addition to the challenge of accurately localizing a moving target, there is a dosimetric concern associated with the interplay effect when employing Intensity Modulated Radiation Therapy (IMRT). This phenomenon can lead to a decrease in the radiation dose delivered to the target volume and an increase in the dose to normal tissue (Jiang et al., 2003).

Various approaches are available to mitigate the influence of respiratory motion, including techniques such as respiratory gating and breath-hold maneuvers, particularly applicable to tumors in the thoracic or abdominal regions (Latty et al., 2015). The fundamental premise underlying respiratory management methodologies is the assumption of a discernible correlation between the target's position and both the phase of respiration and lung volume. This

correlation allows for precise delivery of radiation during imaging and treatment within a specific phase of the patient's breathing cycle (Keall et al., 2006; Stevens et al., 2001).

In this context, the TG 142 guidelines (Klein et al., 2009) advocate the utilization of dynamic phantoms to replicate organ motion induced by respiration. This is crucial for evaluating the precision of target localization and the efficacy of respiratory management techniques. As outlined in the document's protocols, a comprehensive assessment includes evaluating the gating system's ability to consistently reproduce identical respiratory phases during treatment sessions, known as the reproducibility test. Additionally, the accuracy of target positioning during gating is evaluated using dynamic phantoms, referred to as the positioning accuracy test. Furthermore, the AAPM Task Group 290 offers recommendations for assessing the impact of respiratory motion in particle therapy, emphasizing the use of motion phantoms that can realistically replicate the moving anatomy and measuring the delivered dose, which is a critical component of this evaluation process (Li et al., 2022).

Although commercially available respiratory management systems exist (Li et al., 2023), Nano et al. note that current gating or breath-hold motion management methods are often expensive and inaccessible to low-to-middle-income countries (LMICs) (Nano et al., 2020). In this scenario, some in-house systems have been developed with the prerogative of low cost (Farzaneh et al., 2018; Macrie et al., 2015; Nano et al., 2020), rendering them applicable on a wide scale within LMICs. However, it is crucial to develop dynamic phantoms to validate and evaluate these tools for clinical implementation. Therefore, the present study is focused on the development and evaluation of a low-cost dynamic phantom, specifically designed for use in quality assurance for both commercially available and in-house respiratory management systems.

2. Materials and Methods

The phantom's framework was crafted from polycarbonate material, with dimensions of 308 mm in width, 112 mm in height, and 115 mm in depth, as depicted in Figure 1. To induce controlled motion, we employed a Nema 17 Motor, integrated with an A4988 driver and an Arduino UNO board. The motor was powered by a source operating at a nominal output voltage of 12V, while the Arduino received its power from a dedicated power bank with a nominal output voltage of 5V.

To facilitate the precise movement required for simulating respiratory motion, a polycarbonate flat cylinder, resembling a wheel, was directly affixed to the motor shaft, as shown in Figure 1.

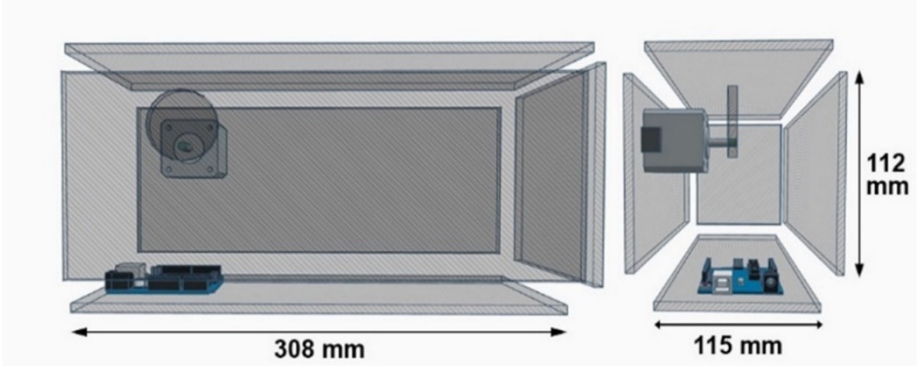

(a)

(b)

Fig. 1. The front and side view of the (a) prototype and of the (b) developed phantom (Illustration developed on the platform https://www.tinkercad.com/things/bTvdIQz3AQy-exquisite-elzing-allis/edit.).

The Arduino was configured using the Arduino Integrated Development Environment (IDE) and the AccelStepper library to execute user-defined motions. These included variables such as cycle count, frequency (movement speed), delay, and amplitude. The Arduino was customized to allow users to specify motion parameters for both free breathing and apnea. For free breathing, these parameters included cycle count and velocity, while for apnea mode, they included cycle count, duration of motion pause, and movement amplitude. Consequently, the dynamic phantom can seamlessly execute a free-breathing motion, wherein the wheel completes a full rotation. Alternatively, it can be programmed to halt at predefined intervals of rotation, pause momentarily, and then revert to its initial position, thus offering users the flexibility to dictate the magnitude of the amplitude. The system's amplitude was modeled by considering the number of steps executed by the motor, contingent on the wheel's radius.

The initial step in modeling the phantom's movement involved calibrating the phantom by quantifying its motion amplitude and monitoring the motor's step count. Motion amplitude was measured every 10 steps throughout a complete cycle, resulting in 20 data points per cycle. This process was repeated six times. The average amplitude data was then correlated with the corresponding step count. To consolidate the findings, a nonlinear regression analysis was subsequently performed on the entire range of phantom motion.

The apnea mode can be executed similarly, with the added flexibility of user-configurable pause durations. Within this mode, users can also fine-tune different amplitudes to suit their requirements. To enhance user-friendliness and streamline interaction with the system, a Graphical User Interface (GUI) was developed for the algorithm. This GUI was developed using the Python programming language, leveraging the Tkinter library.

The structural design of the phantom was developed to accommodate devices used for quality control purposes, including fiducials from the respiratory management system and a radiation detector. To provide a suitable housing for the ionization chamber and ensure the establishment of charged particle equilibrium, a semispherical cap made from paraffin material with a relative density ranging from 0.8 to 0.9 relative to water was employed. This cap had an approximate diameter of 100 mm and incorporated a central cavity parallel to its base, designed to accommodate a PinPoint-type ionization chamber, as illustrated in Figure 1. While the paraffin cap primarily mimics the shape of a breast for specific applications, alternative geometries such as parallelepipeds, semicylinders, and others may also be employed as needed.

To effectively employ the phantom in quality control tests, adhering to the guidelines set forth by AAPM protocols, several critical operational attributes must be evaluated. The validation of the phantom encompassed a series of executed tests. The repeatability of the phantom's movements was rigorously scrutinized under varying conditions of amplitudes and frequencies. Data were collected over ten cycles for various frequencies and amplitudes. In the context of apnea mode, the frequency assessment was conducted by analyzing the repeatability of the apnea duration, simulating a patient in deep inspiration breath hold. Amplitudes of 10, 20, and 30 mm, speeds of 1-4, and their associated frequencies and apnea durations of 5, 10, 20, and 30 seconds were evaluated. To evaluate the system's reproducibility, an analysis was conducted using data from three amplitude and frequency measurements.

To assess the suitability of the simulator for dosimetric testing, a computed tomography (CT) images was performed with a slice thickness of 2 mm. The potential generation of artifacts from the motor, microcontroller, and other components was also examined. Additionally, the density of the build-up layer (paraffin hemisphere) was evaluated using Hounsfield Units (HU).

The data collection process involved recording videos to capture the movements executed by the simulator, which was mounted on a flat surface. The video camera was fixed to a stand. The collected data was processed using the "Tracker" software, a freely available tool for video modeling and analysis (Tracker Community, [s.d.]). This software enabled the selection of a reference point (a sample of pixels) in the video image, followed by the establishment of a coordinate system, and accurate measurement of the position of a designated point on the simulator over time.

To ensure the accuracy of the software, it had been previously calibrated using a caliper that had undergone rigorous calibration by a traceable laboratory. The video recording process was executed with a high-definition (HD) camera boasting a frame rate of 30 frames per second, ensuring the acquisition of precise and high-quality data.

3. Results

The recorded measurements of amplitudes, correlating them with the number of motor steps, underwent thorough data processing, culminating in the formulation of two distinct models. The first model was based on a

Gaussian function, tailored to align with the measured data derived from complete revolutions, totaling 200 steps. Simultaneously, another model was crafted using a nonlinear regression analysis of the data encompassing half a cycle, relying on a third-degree polynomial function. Both modeling approaches yielded coefficients of determination values of 0.99, indicating a strong agreement between the models and the actual dataset. This robust consistency between the calculated models and the empirical observations is illustrated in Figure 2.

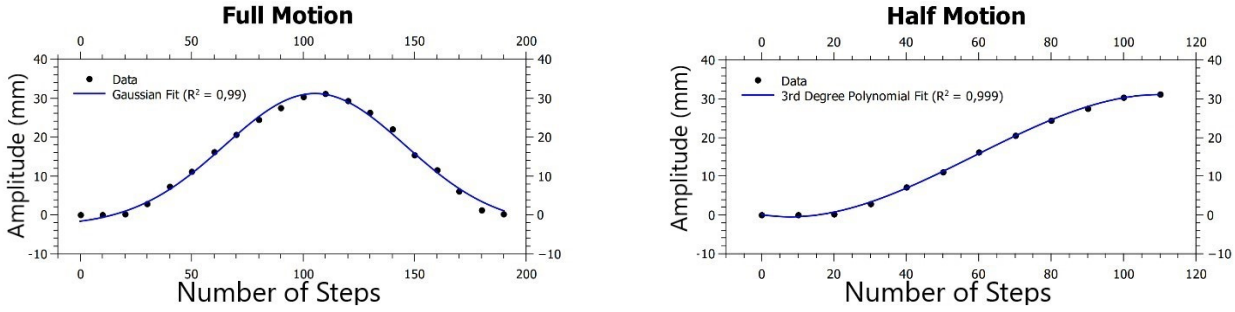

Figure 2. Graph of amplitude as a function of the number of motor steps for **(a)** full motion and **(b)** half motion.

The data recorded during the repeatability tests, covering amplitude, cycle frequency, and apnea duration, were represented graphically in Figures 5 and 6. When the simulator operated in free-breathing mode, it yielded an average amplitude measurement of 31.2 ± 0.17 mm (ranging from 31.06 to 31.18 mm), indicating a global relative deviation of 0.5%. This calculation incorporated data collected across various speeds. A slightly higher deviation of approximately 0.4% was observed in readings taken at speed 4 compared to the average. In contrast, the smallest deviations were noted at speeds 1 and 2, both registering at less than 0.2%.

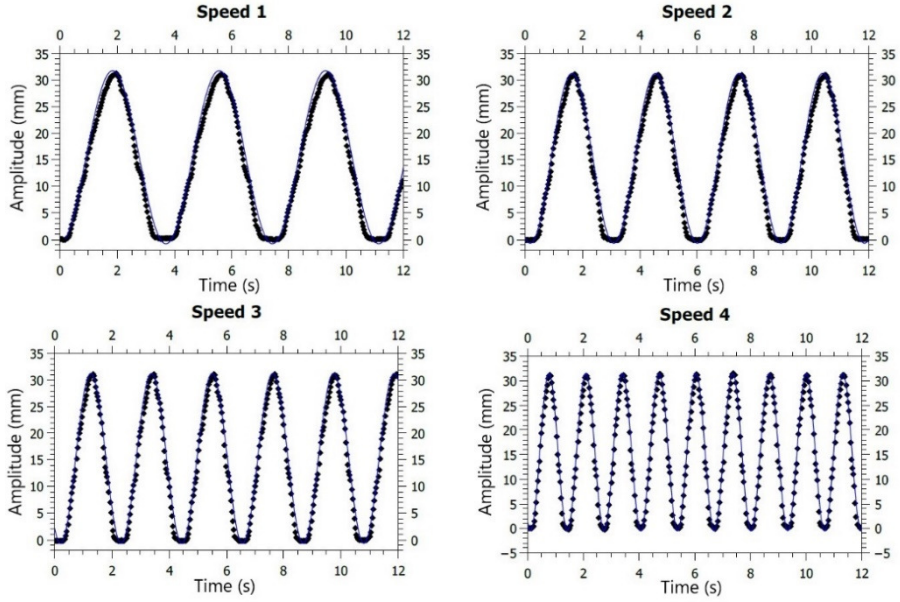

Figure 3. Graphs of the amplitude as a function of time for a free breathing movement of different frequencies. The solid line represents a fit made on the graph.

In the reproducibility test, a variance relative to the mean of less than 0.5% was observed across the widest range examined. The evaluated engine rotation speeds, arranged in ascending order, corresponded to the following frequencies: 0.27 Hz, 0.34 Hz, 0.47 Hz, and 0.75 Hz. Upon evaluation, relative deviations were identified, not exceeding 0.19%, for the same measured frequency.

During the operation of the phantom in apnea mode, the most notable relative variation observed pertained to the suspension time of movement, amounting to a maximum of 0.8%, which corresponded to a difference of 0.32 seconds. Concerning the consistency of amplitudes, a relative deviation of 0.4% was recorded for the maximum height achieved during the motion.

Figure 5 presents the data obtained from the repeatability test of the amplitude, encompassing nominal amplitudes of 10, 20, and 30 mm, all conducted with a fixed apnea time of 1.0 second. It is noteworthy that the measured height for each of these assessed amplitudes is contingent upon the precise moment at which measurements are acquired. Upon an analysis of the collected data, the highest detected variation was 0.6%. This observation underscores the feasibility of conducting consistency tests with the phantom, while accounting for inherent variations in motion that are consistently less than 0.18 mm, particularly for amplitudes exceeding 10 mm.

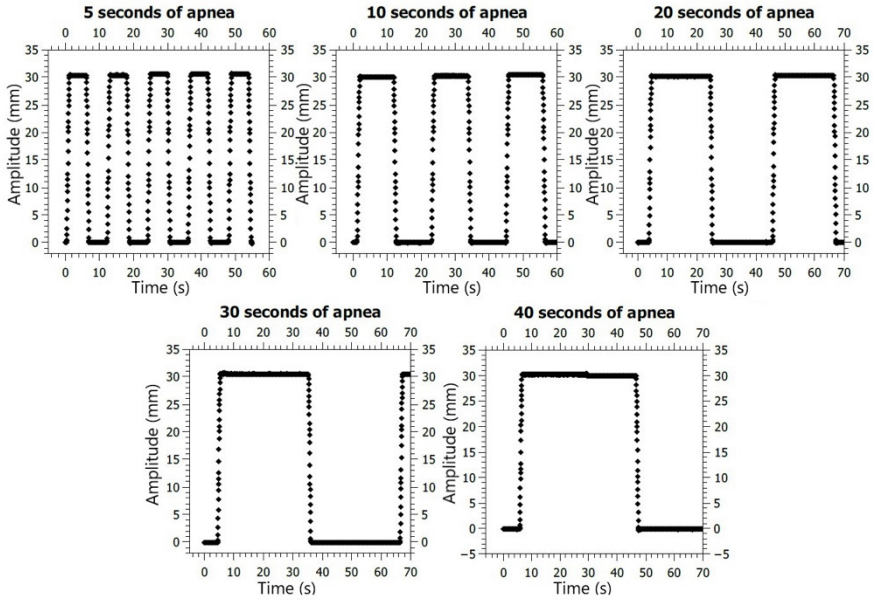

Figure 4. Graphs of the amplitude as a function of time for different apnea durations.

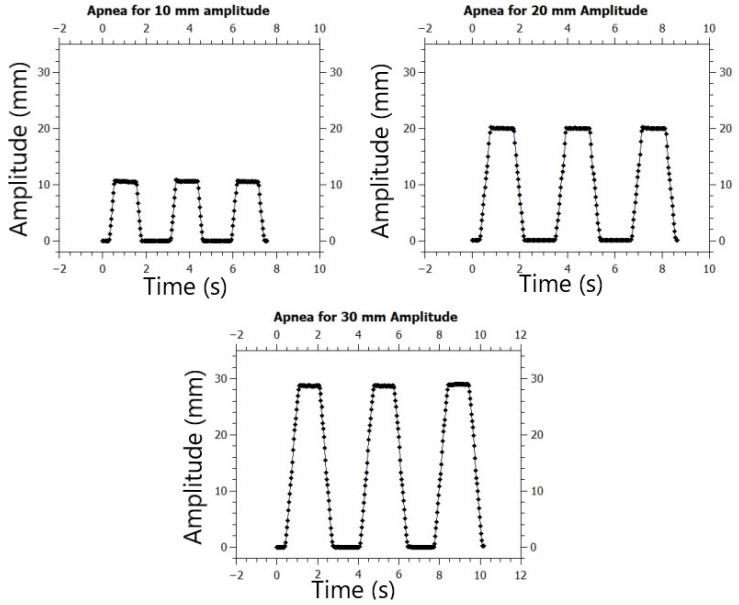

Figure 5. Graphs for the repeatability test for amplitudes of 10, 20, and 30 mm.

The computed tomography (CT) images of the phantom were imported into the Eclipse Treatment Planning System, version 13.6, developed by Varian Medical Systems, based in Palo Alto, CA. A thorough examination of these images revealed the presence of artifacts, primarily originating from components of the stepper motor. Remarkably, these artifacts had no discernible impact on the regions of the slices that encompassed the paraffin cap. Additionally, an average Hounsfield Units (HU) value of -215±40 was determined for the relevant volume within the phantom. The dimensions of the paraffin layer were also adequate to ensure balance of charged particles.

4. Discussion

Breath-hold techniques in radiotherapy, primarily for lung and liver cancers, can also benefit breast cancer treatment by displacing the heart away from the breast during inhalation (Bergom et al., 2018; Bruzzaniti et al., 2013; Duma et al., 2019; Keall et al., 2006; Latty et al., 2015; Wolf et al., 2023). Deep breathing reduces irradiated cardiac and pulmonary volumes (FASSI et al., 2014), advantageous in chemotherapy regimens due to cardiotoxicity risks (Lu et al., 2000; Pedersen et al., 2004; Smyth et al., 2015; Xin et al., 2021). However, respiratory management requires caution; Bright et al., (2022) identified 57 potential failure modes in DIBH for breast cancer.

Cost-effective phantoms are crucial, especially for in-house systems (Farzaneh et al., 2018; Nano et al., 2020). This study aimed to create and validate a phantom for tests mandated by respiratory monitoring protocols, like TG 142 and TG 76 (Keall et al., 2006a; Klein et al., 2009) providing QA insights for respiratory gating.

Dynamic phantoms with radiation detectors can assess dose delivery across respiratory phases, similar to AAPM's Task Group 119 for IMRT (Ezzell et al., 2009). They verify adequate margins for tumor motion (Klein et al., 2009) and evaluate respiratory system response times, critical for high dose-rate FFF beams to prevent overdosing.

Farzaneh et al. (2018) used a dynamic phantom to validate their gating system, but lacked detail on testing modalities. Phantoms for in-house systems must facilitate comprehensive quality control as per TG 142/76. A robust, cost-effective system is essential for thorough QA.

Nonetheless, crafting a phantom that adequately meets all these requirements is a complex undertaking. Existing literature showcases studies that have ingeniously adapted commercial phantoms to incorporate movements and breathing patterns not originally encompassed by the off-the-shelf models (Cheung; Sawant, 2015; Dunn et al., 2012; Ranjbar et al., 2019). The prospect of integrating electronic add-ons to enhance the phantom's degree of freedom holds substantial promise. Moreover, for a comprehensive evaluation of the Treatment Planning System, the phantom must be designed to account for tissue density variations, particularly when addressing scenarios involving pulmonary lesions.

In our study, the developed phantom demonstrated satisfactory results during the development and validation stages. The amplitudes recorded and correlated with motor steps generated a higher coefficient of determination for the third-degree polynomial function. Consequently, the phantom movement was modeled based on this function. During repeatability tests, the simulator operating in free-breathing mode produced an average amplitude measurement of 31.2 ± 0.17 mm, with a global relative deviation of 0.5%. No movement variations greater than 0.18 mm were observed for amplitudes greater than 10 mm. Higher deviations were noted at speed 4 (0.4%) compared to speeds 1 and 2 (<0.2%). Reproducibility tests revealed a variance relative to the mean of less than 0.5%, suggesting a measurement uncertainty of less than 0.5 mm. This aligns with findings from an in-house lung module study (Ranjbar et al., 2019), demonstrating minimal relative deviations in cycle periods (≤0.19%) across frequencies (0.27 Hz, 0.34 Hz, 0.47 Hz, 0.75 Hz). In apnea mode, the maximum relative variation in movement suspension time was 0.8% (0.32 seconds). Amplitude consistency tests showed a maximum variation of 0.6%, indicating reliable performance with variations consistently below 0.18 mm for amplitudes above 10 mm. Regarding the paraffin cap, the average Hounsfield Units (HU) value was -215 ± 40, which is lower than those found for soft and adipose tissue (soft tissue 60 ± 25 and adipose tissue -190 a -30) (Abdollahi et al., 2024; Kvist; Sjöström; Tylén, 1986), but sufficient to promote electronic balance for the measured dose.

According to Reitz et al., 2020, the maximum amplitude (maximum expiration) observed during free breathing in a study evaluating the reproducibility and stability of the DIBH technique in radiotherapy for breast cancer was 15.8 mm, with a range from 8.5 to 30.6 mm (Reitz et al., 2020). Therefore, the developed phantom possesses the ability to replicate the movement observed in real patients, demonstrating its robustness and versatility as a tool for comprehensive quality control tests in respiratory management systems. The phantom’s high precision and reproducibility make it suitable for a variety of assessments, including dosimetric evaluations and the simulation of various respiratory cycles. Despite certain limitations, the phantom is effective for evaluating the overall performance of respiratory management systems, including the response times for beam interruption. It is also useful for dosimetric assessments of the interplay effect, especially with IMRT techniques targeting moving tumors.

Although the phantom proposed in this work provides a comprehensive suite of quality control tests for respiratory management systems, to enhance its practicality and utility further, it would be advantageous to explore the integration of a radiofrequency communication module (wireless), such as the RF24L01. This technological addition could facilitate seamless communication and data transfer, streamlining the integration of the phantom into clinical workflows.

5. Conclusions

Our study underscores the robustness and versatility of the proposed phantom as a valuable tool for performing comprehensive quality control tests in respiratory management systems. Key attributes of this phantom include its high precision and reproducibility. It also enables assessments, including dosimetric evaluations, simulating a variety of respiratory cycles.

However, it's important to note that the phantom's functionality is primarily suited for tests recommended for respiratory management systems, including end-to-end tests. Due to limited movement along the vertical axis and the absence of materials simulating density variations in the human body, it is particularly well-suited for evaluating treatment planning for breast cancer. Notably, it is not suitable for assessing respiratory management systems based on spirometry.

Nevertheless, the phantom can serve as a valuable tool for an overall assessment of respiratory management systems, including the evaluation of response times for beam interruption when applied. Additionally, it finds application in dosimetric assessments of the interplay effect, especially in the context of the IMRT technique applied to moving targets.

Acknowledgments: We express our gratitude to the University Hospital of Brasília, where the tests were conducted.

Conflicts of Interest: There is no conflict of interest.

References

1. Abdollahi, S. et al. Dynamic anthropomorphic thorax phantom for quality assurance of motion management in radiotherapy. **Physics and Imaging in Radiation Oncology**, v. 30, p. 100587, abr. 2024.
2. Bergom, C. et al. Deep inspiration breath hold: Techniques and advantages for cardiac sparing during breast cancer irradiation. **Frontiers in Oncology**, v. 8, n. APR, 4 abr. 2018.
3. Bright, M. et al. Failure modes and effects analysis for surface-guided DIBH breast radiotherapy. **Journal of Applied Clinical Medical Physics**, v. 23, n. 4, 1 abr. 2022.
4. Bruzzaniti, V. et al. Dosimetric and clinical advantages of deep inspiration breath-hold (DIBH) during radiotherapy of breast cancer. **Journal of Experimental and Clinical Cancer Research**, v. 32, n. 1, 2013.
5. Cheung, Y.; SAWANT, A. An externally and internally deformable, programmable lung motion phantom. **Medical Physics**, v. 42, n. 5, 1 maio 2015.
6. Duma, M. N. et al. Heart-sparing radiotherapy techniques in breast cancer patients: a recommendation of the breast cancer expert panel of the German society of radiation oncology (DEGRO). **Strahlentherapie und Onkologie**, v. 195, n. 10, p. 861–871, 1 out. 2019.
7. Dunn, L. et al. A programmable motion phantom for quality assurance of motion management in radiotherapy. **Australasian Physical and Engineering Sciences in Medicine**, v. 35, n. 1, p. 93–100, mar. 2012.
8. Ezzell, G. A. et al. IMRT commissioning: Multiple institution planning and dosimetry comparisons, a report from AAPM Task Group 119. **Medical Physics**, v. 36, n. 11, p. 5359–5373, 2009.
9. Farzaneh, M. J. K. et al. Design and construction of a laser-based respiratory gating system for implementation of deep inspiration breathe hold technique in radiotherapy clinics. **Journal of Medical Signals and Sensors**, v. 8, n. 4, p. 253–262, 1 out. 2018.
10. Fassi, A. et al. Reproducibility of the external surface position in left-breast DIBH radiotherapy with spirometer-based monitoring. **Journal of Applied Clinical Medical Physics**, v. 15, n. 1, p. 130–140, 2014.
11. Jiang, S. B. et al. An experimental investigation on intra-fractional organ motion effects in lung IMRT treatments. **MEDICINE AND BIOLOGY Phys. Med. Biol**, v. 48, p. 1773–1784, 2003.
12. Keall, P. J. et al. **The management of respiratory motion in radiation oncology report of AAPM Task Group 76Medical Physics**. [s.l.] John Wiley and Sons Ltd, 2006.
13. Klein, E. E. et al. **Task group 142 report: Quality assurance of medical accelerators**. **Medical Physics.** John Wiley and Sons Ltd, , 2009.
14. Kvist, H.; SJÖSTRÖM, L.; TYLÉN, U. Adipose tissue volume determinations in women by computed tomography: technical considerations. **International journal of obesity**, v. 10, n. 1, p. 53–67, 1986.
15. Latty, D. et al. Review of deep inspiration breath-hold techniques for the treatment of breast cancer. **Journal of Medical Radiation Sciences**, v. 62, n. 1, p. 74–81, 1 mar. 2015.

16. Li, H. et al. AAPM Task Group Report 290: Respiratory motion management for particle therapy. **Medical Physics**, v. 49, n. 4, 31 abr. 2022.
17. Li, N. et al. Design of a Patient-Specific Respiratory-Motion-Simulating Platform for In Vitro 4D Flow MRI. **Annals of Biomedical Engineering**, v. 51, n. 5, p. 1028–1039, 29 maio 2023.
18. Lu, H.-M. et al. **REDUCTION OF CARDIAC VOLUME IN LEFT-BREAST TREATMENT FIELDS BY RESPIRATORY MANEUVERS: A CT STUDY**. 2000.
19. Macrie, B. D. et al. A cost-effective technique for cardiac sparing with deep inspiration-breath hold (DIBH). **Physica Medica**, v. 31, n. 7, p. 733–737, 1 nov. 2015.
20. Nano, T. et al. OpenABC: An Open-Source Active Breathing Control System for Low-Resource Centers. **International Journal of Radiation Oncology*Biology*Physics**, v. 108, n. 3, p. e388, nov. 2020.
21. Pedersen, A. N. et al. Breathing adapted radiotherapy of breast cancer: Reduction of cardiac and pulmonary doses using voluntary inspiration breath-hold. **Radiotherapy and Oncology**, v. 72, n. 1, p. 53–60, jul. 2004.
22. Ranjbar, M. et al. A novel deformable lung phantom with programably variable external and internal correlation. **Medical Physics**, v. 46, n. 5, p. 1995–2005, 1 maio 2019.
23. Reitz, D. et al. Stability and reproducibility of 6013 deep inspiration breath-holds in left-sided breast cancer. **Radiation Oncology**, v. 15, n. 1, p. 121, 24 dez. 2020.
24. Shirato, H. et al. Intrafractional Tumor Motion: Lung and Liver. **Seminars in Radiation Oncology**, v. 14, n. 1, p. 10–18, 2004.
25. Smyth, L. M. et al. The cardiac dose-sparing benefits of deep inspiration breath-hold in left breast irradiation: A systematic review. **Journal of Medical Radiation Sciences**, v. 62, n. 1, p. 66–73, 1 mar. 2015.
26. Stevens, C. W. et al. **RESPIRATORY-DRIVEN LUNG TUMOR MOTION IS INDEPENDENT OF TUMOR SIZE, TUMOR LOCATION, AND PULMONARY FUNCTION**. 2001.
27. Tracker COMMUNITY. **Tracker Video Analysis and Modeling Tool**. Disponível em: <https://physlets.org/tracker/>. Acesso em: 27 maio. 2024.
28. Wolf, J. et al. Deep inspiration breath-hold radiation therapy in left-sided breast cancer patients: a single-institution retrospective dosimetric analysis of organs at risk doses. **Strahlentherapie und Onkologie**, v. 199, n. 4, p. 379–388, 1 abr. 2023.
29. Xin, X. et al. Retrospective Study on Left-Sided Breast Radiotherapy: Dosimetric Results and Correlation with Physical Factors for Free Breathing and Breath Hold Irradiation Techniques. **Technology in Cancer Research and Treatment**, v. 20, 2021.